# $\beta$-Limit Investigation in a Straight Stellarator using NIMROD

Mark Schlutt, Chris C. Hegna, and Carl R. Sovinec
University of Wisconsin

Eric D. Held
Utah State University

Scott E. Kruger
Tech-X Corporation


Saturday, April 30, 2011

# Motivation - Calculating the structure of finite-$\beta$ 3D magnetic equilibria is not straightforward.

- Good flux surfaces are not guaranteed to exist in 3D configurations.
- The equations of MHD equilibrium do not allow for stochastic regions to support a pressure gradient: $\mathbf{B} \cdot \nabla p = 0$.
- Notions of equilibrium and stability become blurred.
  - For example, in a resistive MHD model, *equilibrium* island widths depend on parameters related to *stability*.
- **As $\beta$ increases, the magnetic topology changes.**

$=>$ This motivates using a time-dependent extended MHD code to model the 3D equilibrium.

## A model is created to compare helically symmetric cases to spoiled-symmetry cases.

Two classes of equilibria are heated and compared:

1. Vacuum magnetic field is **helically symmetric**
   - fully described by only 2 coordinates (2D): $\vec{B} = \vec{B}(\psi, M\theta - N\zeta)$
   - good closed flux surfaces guaranteed to exist
2. Vacuum magnetic field has **spoiled symmetry**
   - fully 3D magnetic topology
   - closed flux surfaces NOT guaranteed
   - The strength of the symmetry-spoiling harmonics is varied:

$$\epsilon_{mn} = \frac{b_{mn}}{B_0} = 10^{-4}|B_0| \rightarrow 10^{-2}|B_0|.$$

$=>$ **the effect of symmetry-spoiling strength on $\beta$ is investigated**

## NIMROD is used to study the finite-$\beta$ response of these equilibria.

Three different vacuum magnetic configurations are created and studied.

$$\iota(0) \approx 0.34$$

$$\iota(0) \lesssim 0.5$$

$$\iota(0) \gtrsim 0.5$$

- Each of these equilibria is heated at various rates, creating finite-$\beta$ equilibria.
- Anisotropic heat conduction is employed with

$$\chi_{\parallel}/\chi_{\perp} = 10^5 \rightarrow 10^7$$

- The system is perturbed by launching a shear Alfén wave at t=0.

# Straight Stellarator Parameters and Figures of Merit.

All calculations take place in straight stellarator geometry where:

| |
|---|
| $a$ = minor radius $\simeq$ 0.2m |
| $B_0$ = Guide field in axial direction = 1 T |
| $T_{bckgrd}$ = background temperature (at plasma edge) = 1 eV |
| Kinematic viscosity = 1 m$^2/s$ |
| Electrical Diffusivity $(\eta/\mu_0)$ = 1 m$^2/s$ |
| $\tau_E$ = Energy confinement time = $6.9 \cdot 10^{-3}$ s |
| $S$ = Lundquist number = 175,000 |
| $V_A$ = Alfven speed = $8.8 \cdot 10^6$ m/s |
| $\chi_\perp$ = perpendicular thermal diffusivity = 1 m$^2/s$ |
| $\chi_\parallel$ = parallel thermal diffusivity, varied from = $10^5$ m$^2/s$ to $10^7$ m$^2/s$ |
| $P_m$ = magnetic Prantdl number = 1 |

# The (m=2,n=2,$\epsilon$=.75) case is studied.

- Core rotational transform: $\iota(0) = 0.338$.
- Symmetry-spoiling harmonics: (m=5,n=1); (m=6,n=1).
- Heating for this case is broad - "tent shape" - peak at the center to 0 at LCFS in vacuum at each point in the domain.
- Heating profile rotates with the shape of the plasma: n=2.

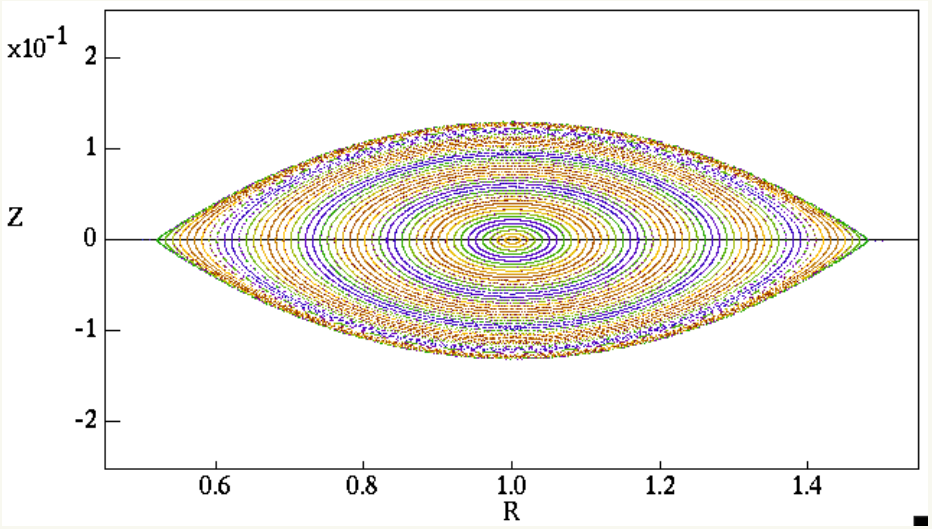


Figure 1: Poincare plot for the helically symmetric case at t=0, $\zeta = 0$.

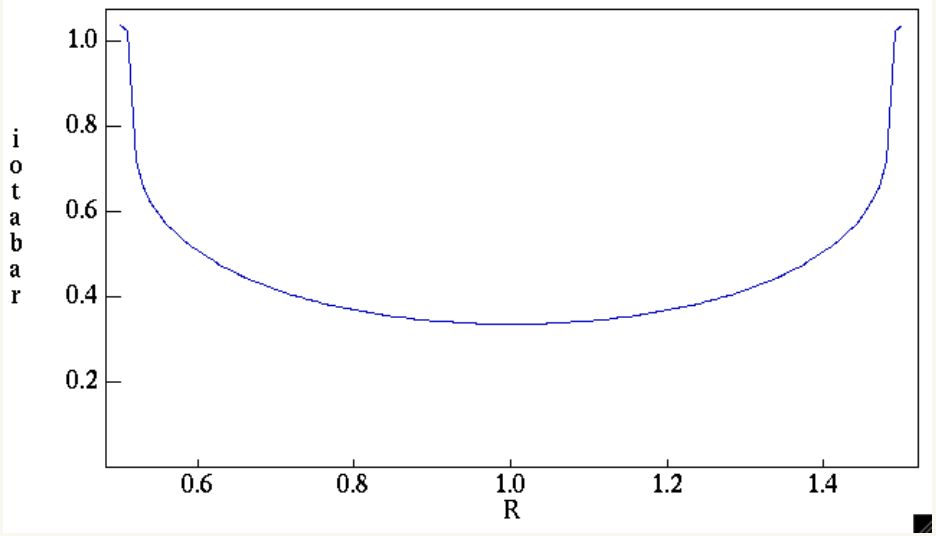


Figure 2: Rotational transform profile at t=0, $\zeta = 0$.



THE UNIVERSITY of WISCONSIN MADISON

# The (m=2,n=2,$\epsilon$=.75) cases disrupt regardless of symmetry-spoiling harmonic strength.

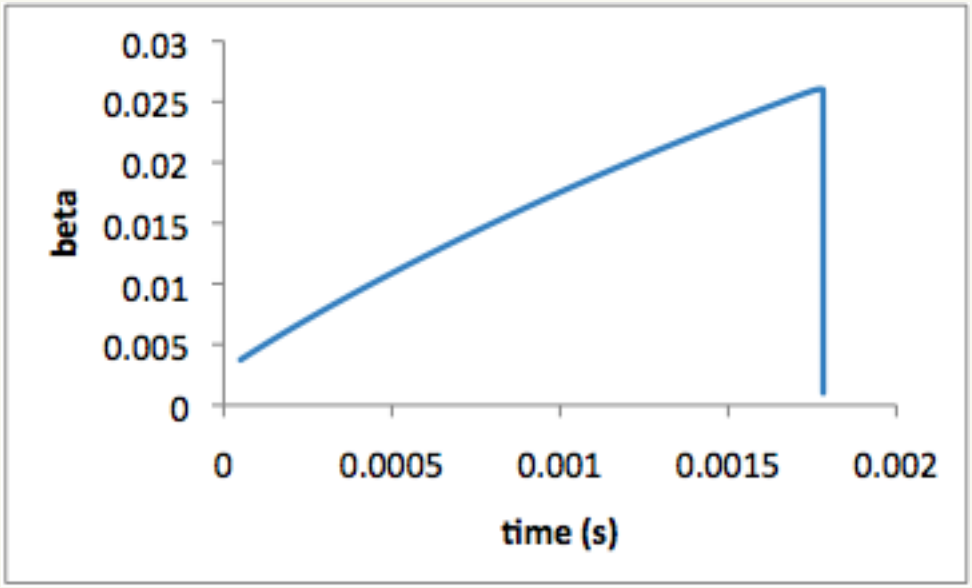


Figure 3: 2D case, (m=2,n=2,$\epsilon$=.75).

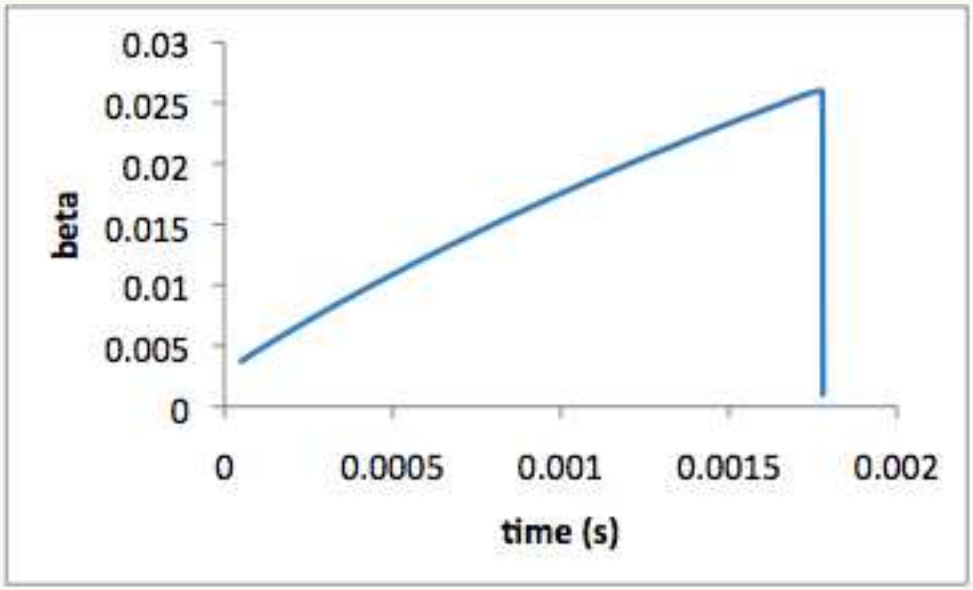


Figure 4: Symmetry-spoiling harmonic strength = $10^{-2}$.

- Both cases: $\beta_{\text{max}} = 2.60\%$ at 1.78 ms.
- These cases are created with moderate heating. Similar results are observed for higher heating rates(x2) and lower heating(1/2) rates.

# The (m=2,n=2,$\epsilon$=.75) cases disrupt regardless of symmetry-spoiling harmonic strength.

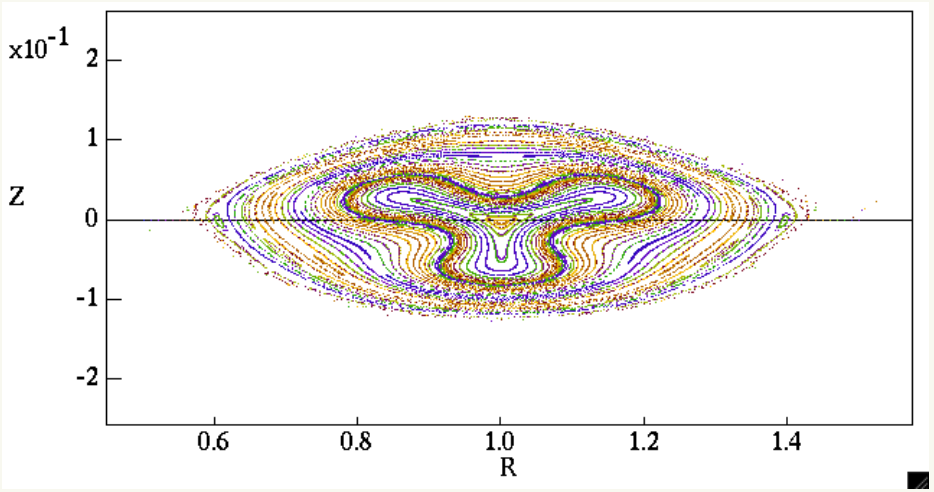


Figure 5: Poincare plot for the helically symmetric case at t=1.72ms, $\zeta = 0$.

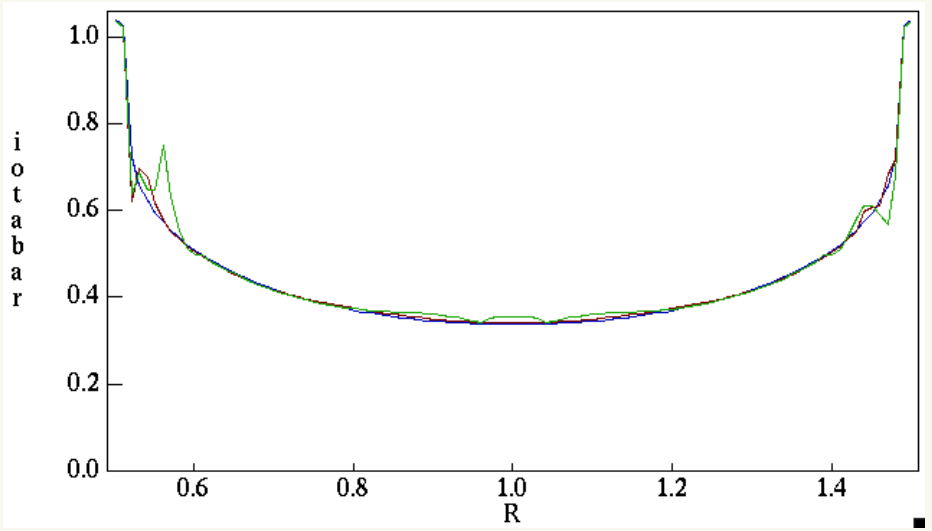


Figure 6: Rotational transform profile at various times, $\zeta = 0$.

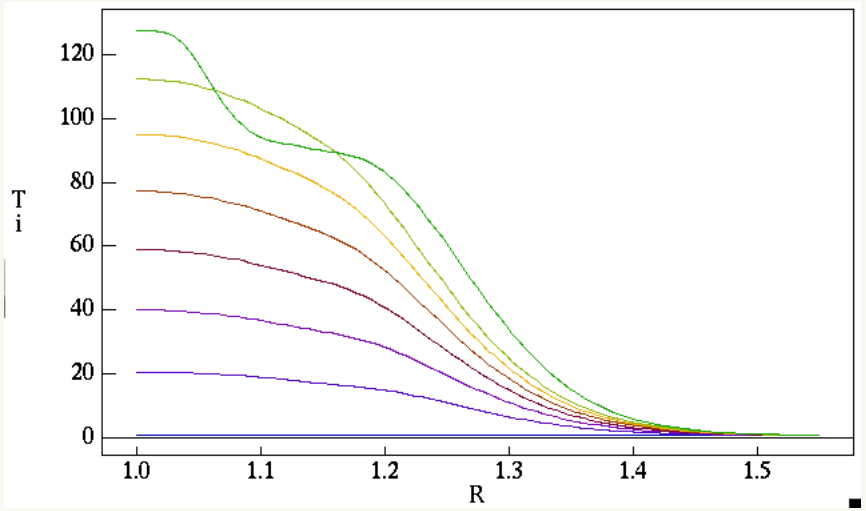


Figure 7: Temperature profiles at various times, $\zeta = 0$.

- The spoiled-symmetry case disrupts in a similar manner - the growth of a core mode.



THE UNIVERSITY of WISCONSIN MADISON

# The (m=2,n=2,$\epsilon$=.87) case is studied.

- Core rotational transform: $\iota(0) = 0.507$.
- Symmetry-spoiling harmonics: (m=5,n=1); (m=6,n=1); (m=6,n=5)
- Heating for this case is broad - "tent shape" - peak at the center to 0 at LCFS in vacuum at each point in the domain.
- Heating profile rotates with the shape of the plasma: n=2.

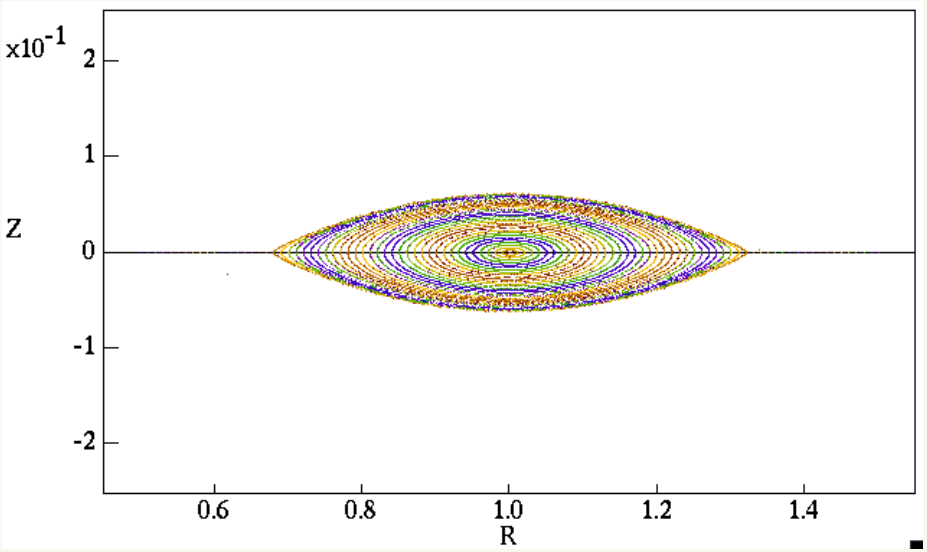


Figure 8: Poincare plot for the helically symmetric case at t=0, $\zeta = 0$.

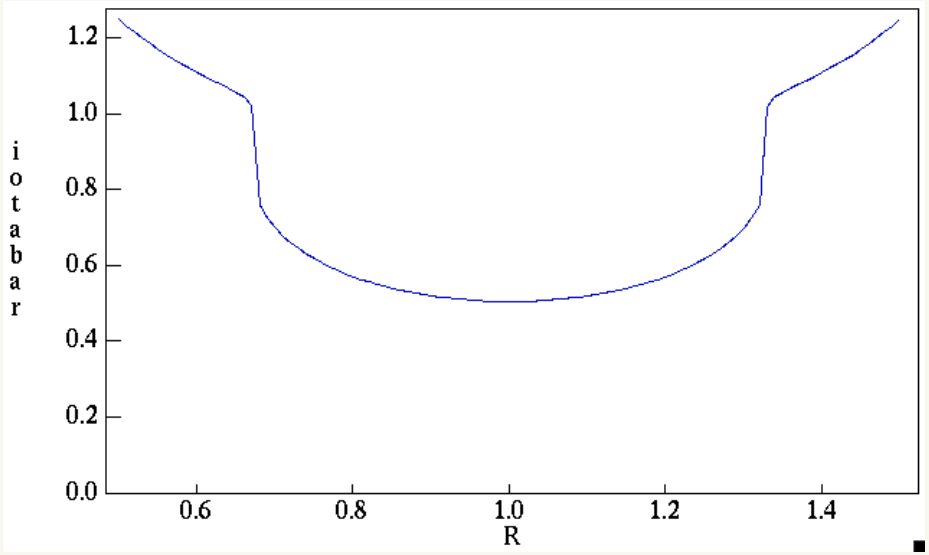


Figure 9: Rotational transform profile at t=0, $\zeta = 0$.



THE UNIVERSITY of WISCONSIN MADISON

# The presence of symmetry-spoiling harmonics delays high-$\beta$ disruption in the (m=2,n=2,$\epsilon$=.87) cases.

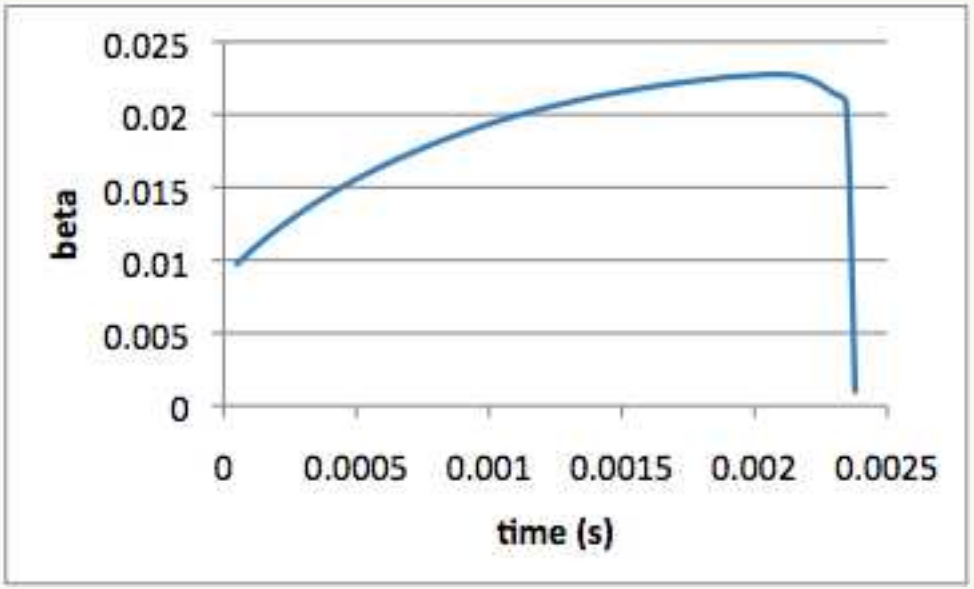


Figure 10: 2D case, (m=2,n=2,$\epsilon$=.87).

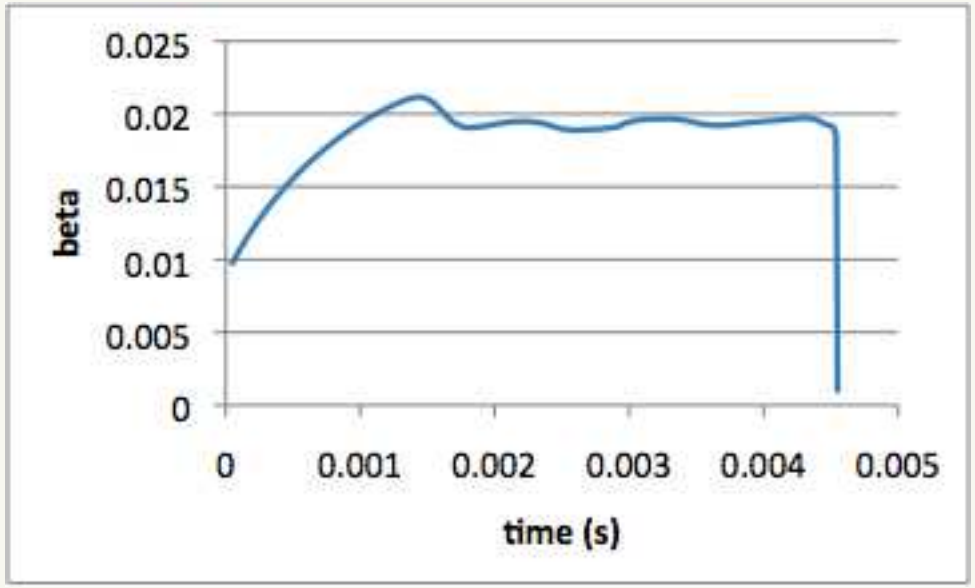


Figure 11: Symmetry-spoiling harmonic strength $= 10^{-2}$.

- 2D case: $\beta_{\text{max}} = 2.28\%$ at 2.10ms. Simulation stops at **2.35ms**.
- Spoiled-symmetry case: $\beta_{\text{max}} = 2.115\%$ at 1.40ms. Simulation stops at **4.54ms**.

# The helically symmetric (m=2,n=2,$\epsilon$=.87) case develops a core mode and quickly disrupts

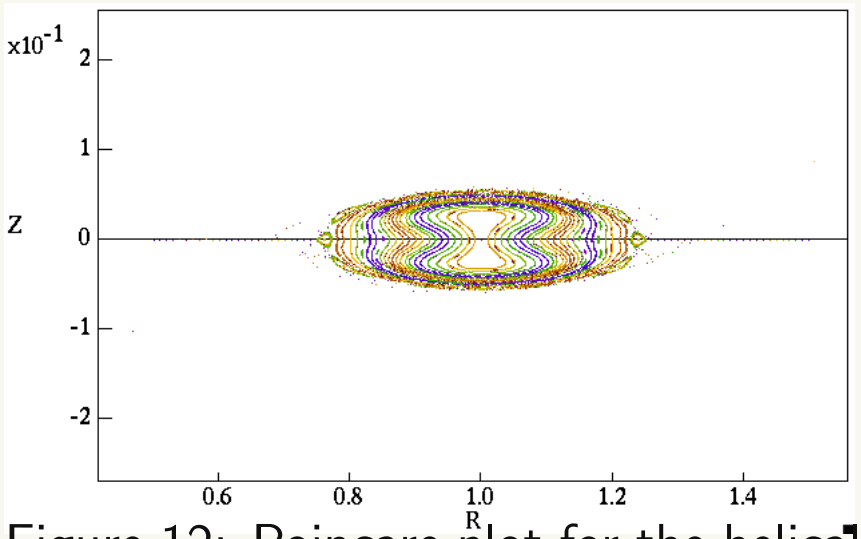


Figure 12: Poincare plot for the helically symmetric case at t=1.72ms, $\zeta = 0$.

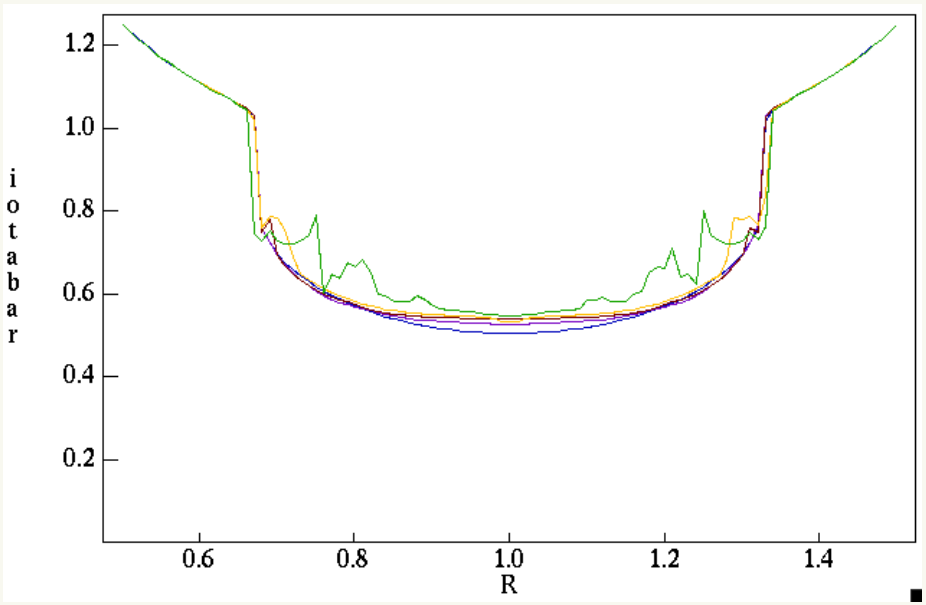


Figure 13: Rotational transform profile at various times, $\zeta = 0$.

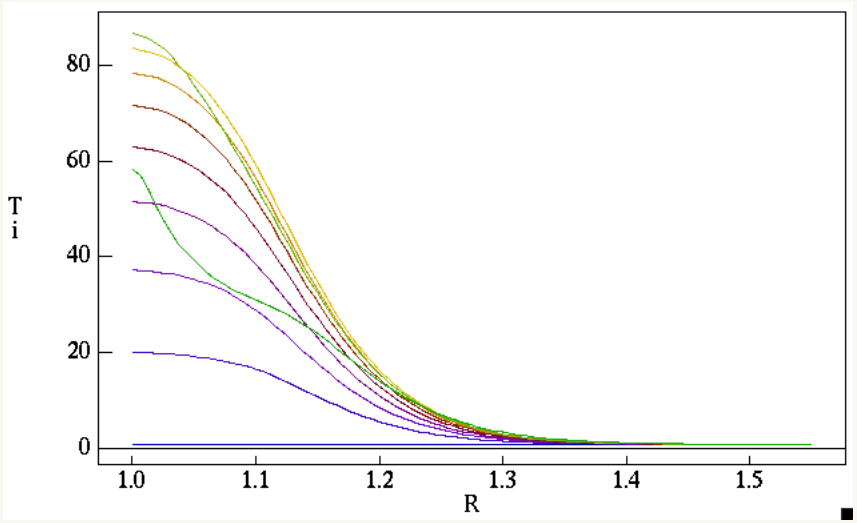


Figure 14: Temperature profiles at various times, $\zeta = 0$.

## Helically Symmetric Case

- Here, a core mode develops which quickly destroys the plasma

# The spoiled-symmetry (m=2,n=2,$\epsilon$=.87) case is more robust.

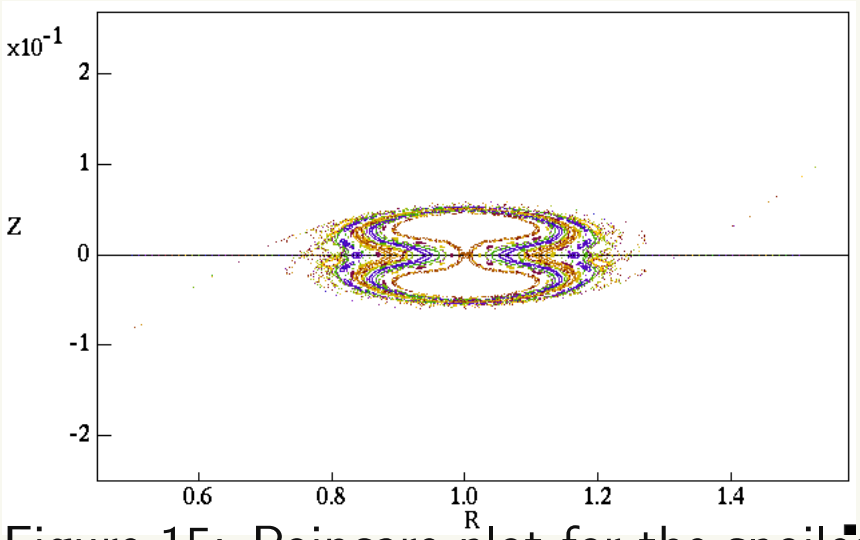


Figure 15: Poincare plot for the spoiled-symmetry case at t=1.50ms, $\zeta = 0$.

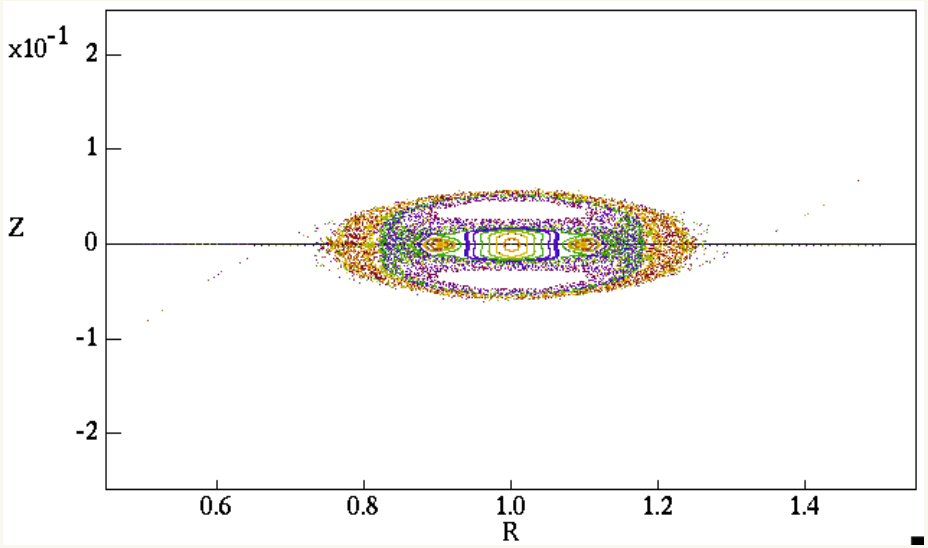


Figure 16: Poincare plot for the spoiled-symmetry case at t=2.55ms, $\zeta = 0$.

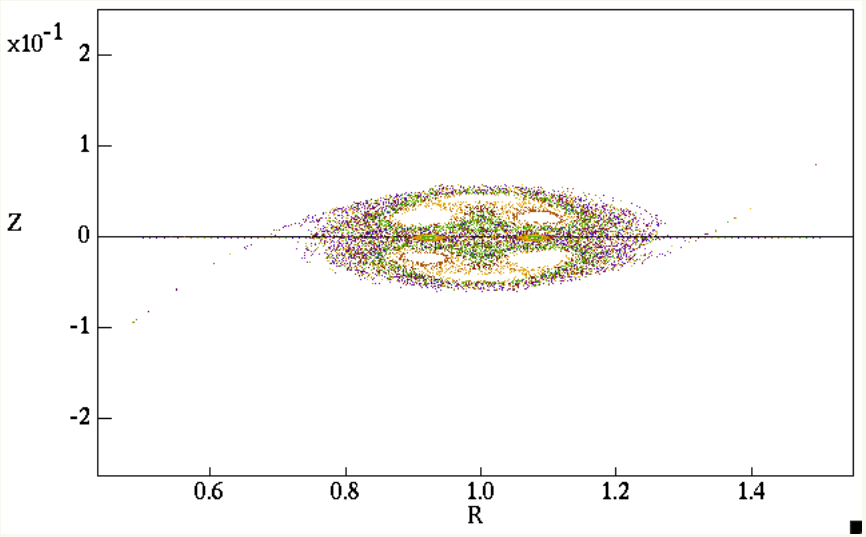


Figure 17: Poincare plot for the spoiled-symmetric case at t=4.53ms, $\zeta = 0$.

## Spoiled Symmetry Case.

- Here, a core mode develops, but the magnetic configuration is robust and recovers the original shape.
- This new equilibrium is dynamic, oscillating between some closed flux surfaces and stochastic fieldlines.

# The spoiled-symmetry (m=2,n=2,$\epsilon$=.87) case is more robust.

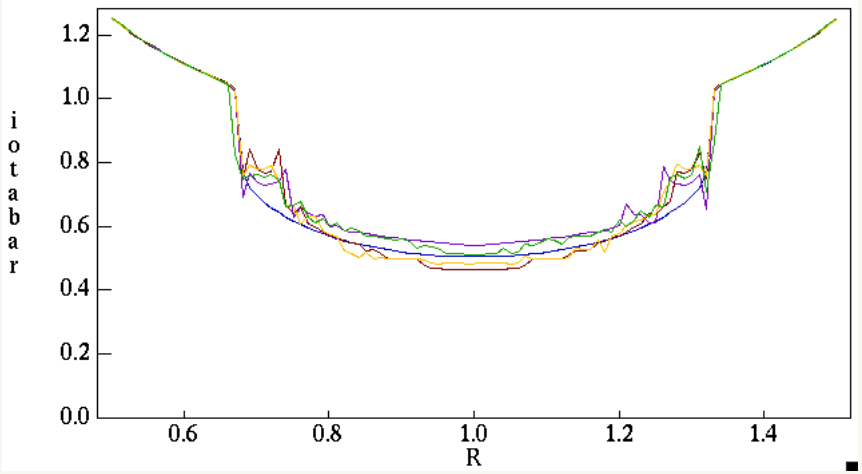


Figure 18: Rotational transform profile at various times, $\zeta = 0$.

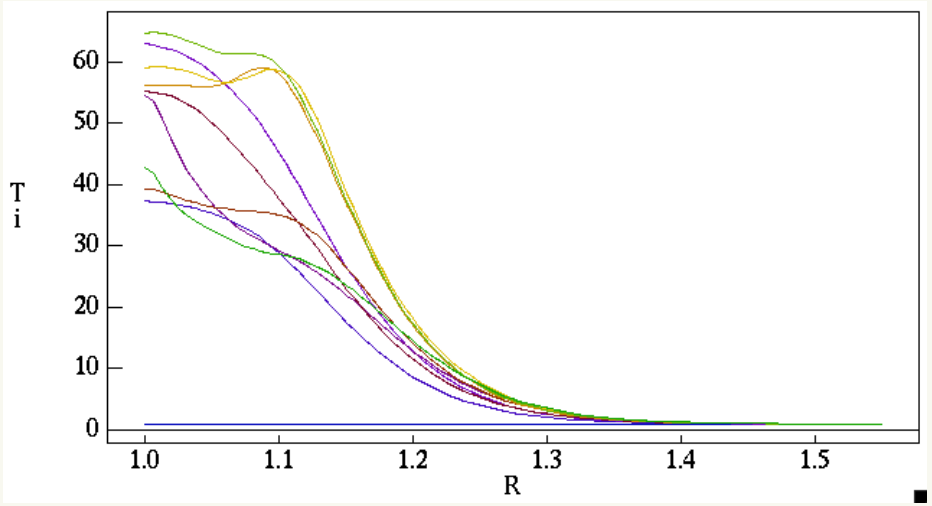


Figure 19: Temperature profiles at various times, $\zeta = 0$.

## Spoiled Symmetry Case.

- The rotational transform profile rises at first (diamagnetism). Then when the core mode develops, the profile drops to $\iota = 0.5$.
- At first the temperature profile deteriorates from the outside in, but then adopts a flat profile which rises with time.

# Increasing $\chi_{\|}$ results in an even more robust configuration.

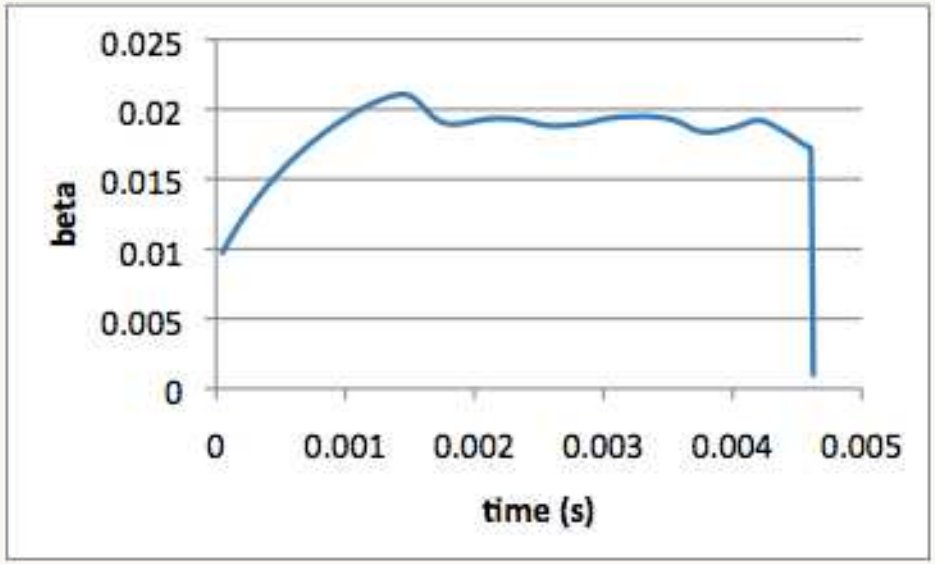


Figure 20: $\chi_{\|} = 10^7$, symmetry-spoiling strength $= 10^{-2}$.

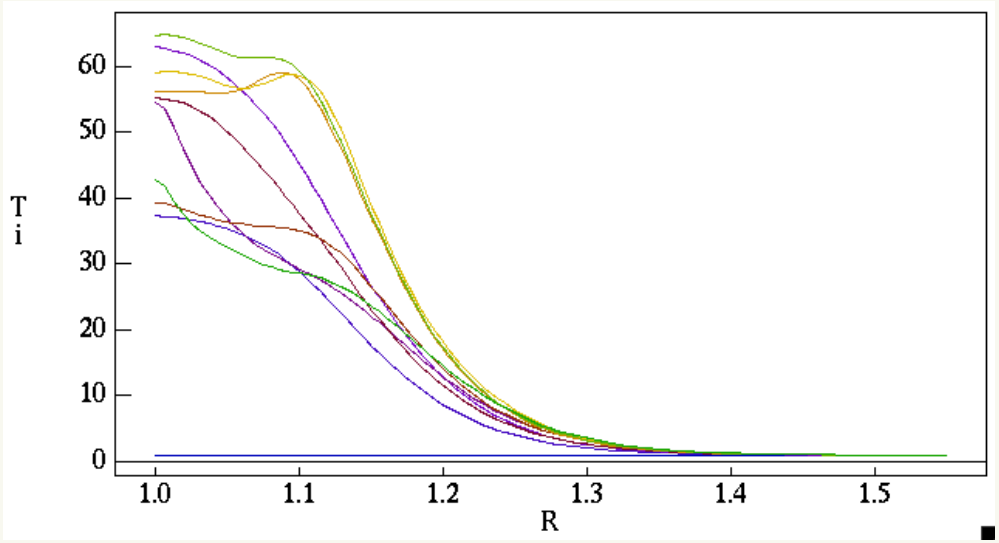


Figure 21: Temperature profiles at various times, $\zeta = 0$.

- The previous spoiled symmetry configuration (m=2,n=2,$\epsilon$=0.87) was restarted from $t = 1.05$ms, but with $\chi_{\|} = 10^7$ (rather than $10^6$).
- $\beta_{\text{max}} = 2.107\%$. Simulation ran until 4.61ms.
- Lower $\beta_{\text{max}}$ and longer runtime as compared with the original spoiled-symmetry configuration.
- Similar behavior as the system is heated, but the flat (or hollow profile) appears sooner.

# Decreasing $\chi_{\|}$ results in a less robust configuration.

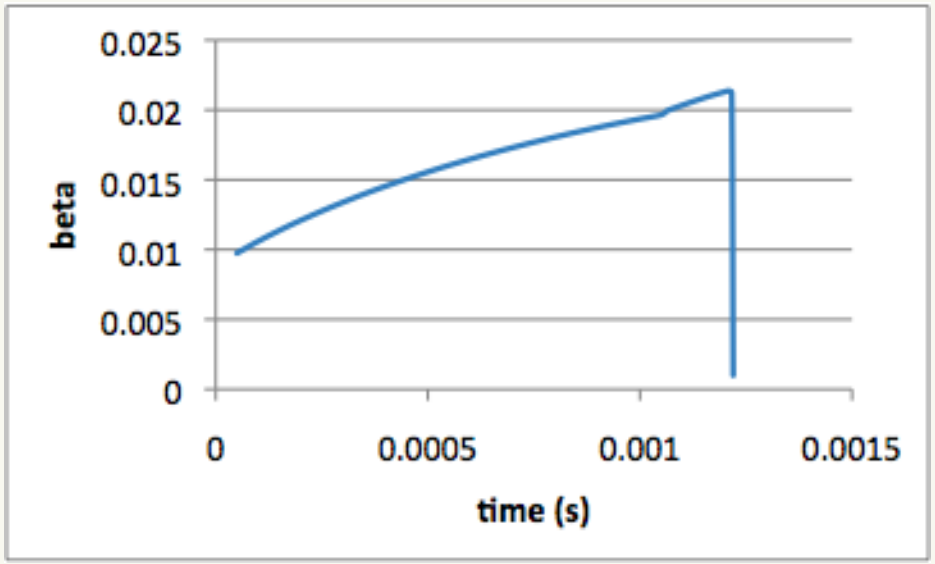


Figure 22: $\chi_{\|} = 10^5$, symmetry-spoiling strength $= 10^{-2}$.

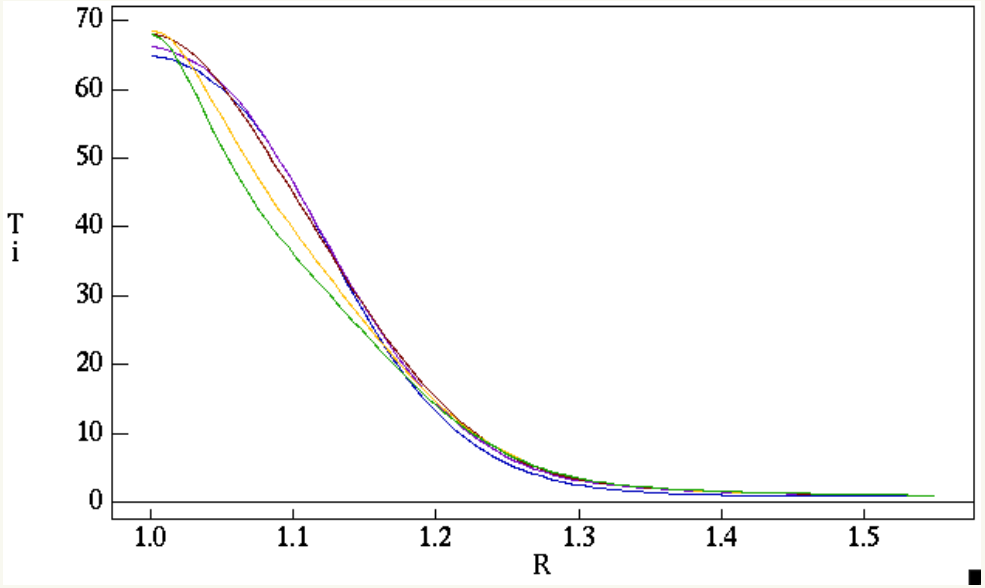


Figure 23: Temperature profiles at various times, $\zeta = 0$.

- The previous spoiled symmetry configuration (m=2,n=2,$\epsilon$=0.87) was restarted from $t = 1.05$ms, but with $\chi_{\|} = 10^5$ (rather than $10^6$).
- $\beta_{\text{max}} = 2.124\%$. Simulation ran until 1.22ms.
- Higher $\beta_{\text{max}}$ and shorter runtime as compared with the original spoiled-symmetry configuration.
- This system's behavior more closely matched the helically symmetric case.

## Summary of these simulations:

Cases with $t_{\text{vacuum}}(0) < 0.5$:

- Both the helically symmetric and spoiled-symmetry systems behaved similarly, regardless of heating rate. All of these cases were run with $\chi_{\parallel} = 10^6$.

Case with $t_{\text{vacuum}}(0) > 0.5$:

- The spoiled-symmetry case was more robust to disruption than the helically symmetric case.
- Changing $\chi_{\parallel}$ affects both $\beta_{\text{max}}$ and the total run time.

## Possible explanation of this phenomenon.

Small stochastic field at the edge acts to limit the pressure gradient that can build. Note that a pressure gradient **does indeed exist** in the **stochastic** region.

- Limits the drive for an interchange instability. A kind of safety valve, so that too much pressure doesn't build.
  - Appears to prevent the onset of edge-resonant modes.
  - Changing $\chi_{\|}$ lowers/raises the pressure gradient that the stochastic region can support.
    - Lower $\chi_{\|}$ => larger pressure gradient in stochastic region => effects of instability are magnified.
    - Higher $\chi_{\|}$ => smaller pressure gradient in stochastic region => effects of instability are mitigated.
- However, this edge stochasticity does not affect the formation of core modes.

# Future Work.

- Further explore the possible combinations:
  - Degree of anisotropic heat conduction - to date have only used $10^5 \leq \chi_{\parallel}/\chi_{\perp} \leq 10^7$.
- Identify the mode structure of the instabilities.
  - Code has been written which analyzes the harmonic structure of the Pfirsch-Schlüter spectrum in helical space.
  - Code is being developed that analyzes $\mathbf{v} \cdot \nabla\psi$ and $\mathbf{b} \cdot \nabla\psi$.
- Perform a $\beta$-scan, where the critical $\beta$ which triggers instability is more accurately determined for these cases.
- Adjust $\chi_{\parallel}$ to investigate the effect of varying the allowable pressure gradient that the stochastic region can support. Determine the relation between $\chi_{\parallel}$ and $\beta$max.

# More Future Work.

Recent work shows a relationship between poloidal rotation and island dynamics in stellarators. See Narushima, et al. in Contributions to Plasma Physics, August 2010, and C.C. Hegna, Poster 2P18 in this poster session.

- Locked islands spontaneously disappear when subjected to large enough poloidal rotation.
- There appears to be hysteresis in the flow/island width evolution.

The current NIMROD straight stellarator model offers a good platform to study these physics.

=> Code development has begun to allow for a poloidal flow source near a vacuum magnetic island.

# The vacuum magnetic field of the Compact Toriodal Hybrid is modeled with NIMROD.

- Magnetic field data at the vessel surface has been provided by the CTH team.
- This data file is read. These data are then converted into NIMROD's Fourier coefficients, and loaded into the boundary finite element nodes.
- nimset is run, producing a configuration with the boundary magnetic field set. Note that Br at this boundary is fixed for all time.
- The magnetic diffusivity is set to a very high value $(10^9)$ and nimrod is run with very short time steps. The goal is to allow the surface magnetic field to diffuse into the domain in a very short amount of time $\sim 10^{-9}$s.
- At this point magnetic diffusivity can be set back to a typical value and the standard types of NIMROD investigations can be performed.

# Poincare Plots of CTH model show closed magnetic flux surfaces.

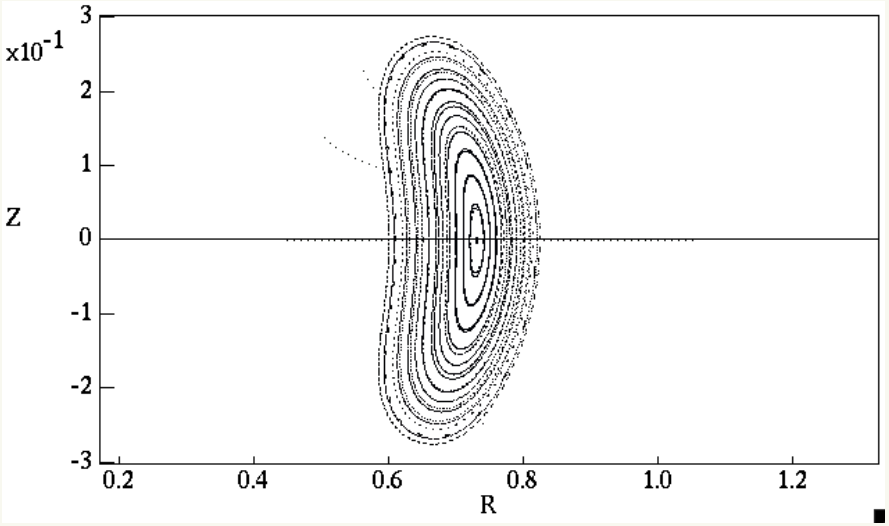


Figure 24: Poincare plot at $\zeta = 0$.

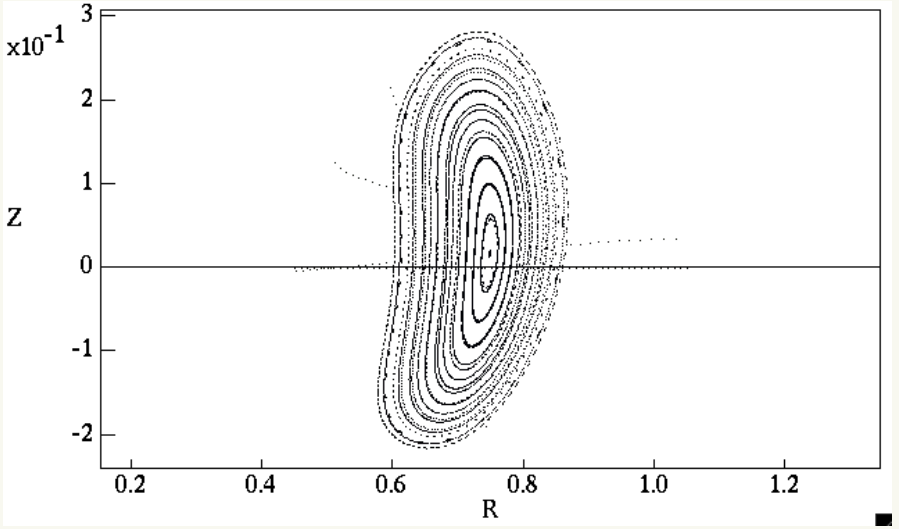


Figure 25: Poincare plot at $\zeta = \pi/10$.

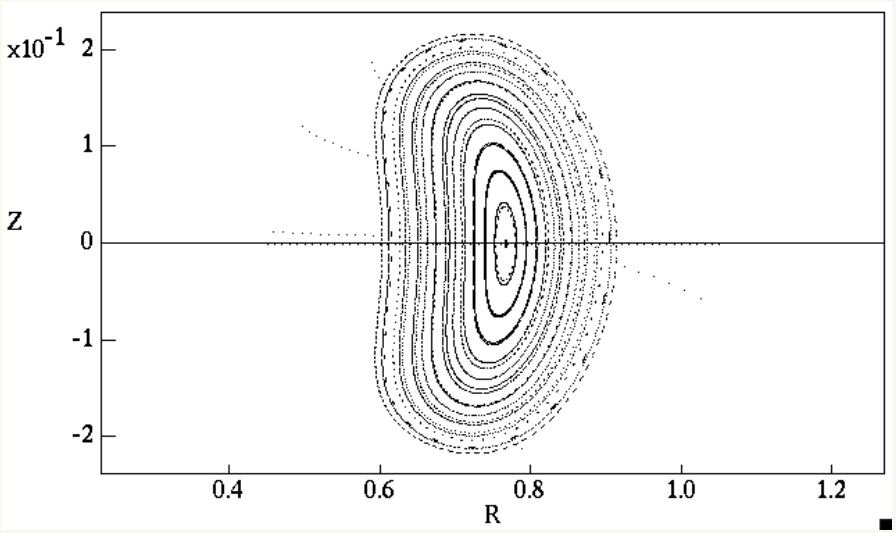


Figure 26: Poincare plot at $\zeta = 2\pi/10$.

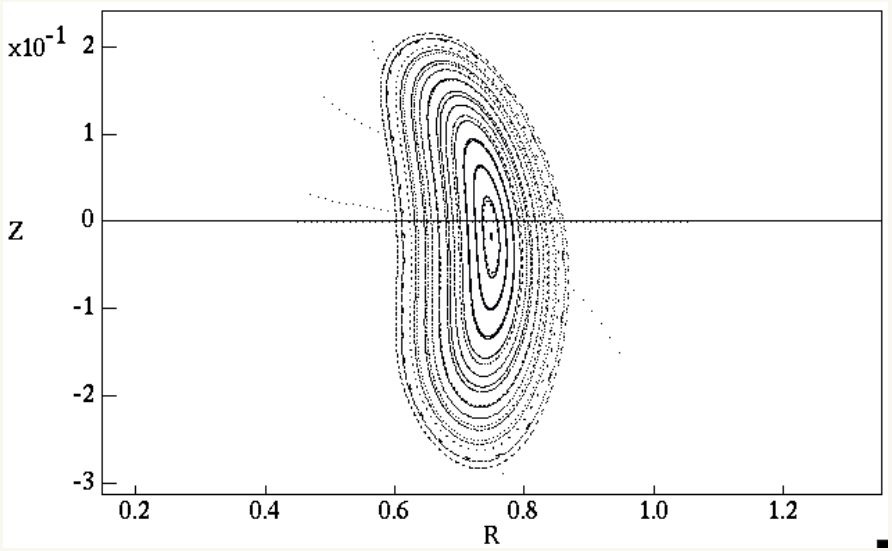


Figure 27: Poincare plot at $\zeta = 3\pi/10$